Journal of Materials Synthesis and Processing, Vol. 6, No. 1, 1998

Effect of Sol-Gel Processing Parameters on Optical Properties of TMOS Silica Aerogels

A. Venkateswara Rao,[1,3] G. M. Pajonk,[2] D. Haranath,[1] and P. B. Wagh[1]

To optimize and produce silica aerogels with high direct transmittance and low diffusive values, systematic and detailed experiments were carried out on the effect of sol-gel processing parameters on optical properties of silica aerogels. A series of aerogel samples of different molar ratio combinations was optically examined in the UV–visible–NIR range by a spectrophotometer equipped with an integrating sphere. The overall transmittance of the aerogels in the visible range varied from 75 to 93% depending upon the molar ratio combination. The most relevant parameter being studied was the direct/hemispherical transmittance ratio (τ). The best value of τ obtained for an aerogel in the present study was about 93% with a molar ratio of 1 TMOS : 12 MeOH : 4 H_2O : 3.5 $\times$ 10^{-3} NH_4OH, respectively. Apart from visible transparencies, solar energetic transparencies of some silica aerogels were also measured and reported. These optical data, together with the porosity measurements, allowed us to improve the process of fabrication of low-diffusing aerogel material. The experimental results are discussed considering the percentage of porosity and heterogeneity generated in pore size distributions due to the variation of sol-gel processing parameters.

KEY WORDS: Silica aerogel; optical transmittance; spectrophotometry; pore size distribution; aerogel windows.

1. INTRODUCTION

During the past few years there has been an increased interest in silica aerogel as a transparent/translucent superinsulating filler for window systems. The development of such a technology is highly significant in that it possesses the potential to revolutionize the building industry worldwide. Also, the widest practical application of transparent silica aerogel as a radiator [1–3] has considerably simplified the construction of Cerenkov counters used in high-energy physics experiments. Refractive indices that would have been possible only with pressurized gases or gases at cryogenic temperatures are now available with silica aerogel. It is the lightest solid medium available to date with the lowest refractive index (~ 1.01) and sufficiently high optical transparency ($\sim 93\%$ at 800 nm) for its utilization in Cerenkov radiation detectors. Even though the market is very limited in this case, there is a need to develop aerogels with the lowest possible index of refraction. It seems that optical properties have been less investigated, probably because the first and foremost applications of silica aerogels were directly related not to the quality of the transparency but to the refractive index. For most applications, a good optical-quality aerogel free of cracks and with a high optical transparency is needed [4]. Although silica aerogels are known for their high optical transparencies, a part of the transmitted visible radiation is diffused, depending upon the sol-gel processing conditions. The diffuse scattering of light not only restricts the construction of aerogel Cerenkov radiation detectors to the threshold type but also decreases

[1] Air Glass Laboratory, Department of Physics, Shivaji University, Kolhapur 416 004, India.

[2] Laboratorie d'Application de la Chimie a l'Environment, Universite Claude Bernard, Lyon I, UMR CNRS 5634, 43 Boulevard du 11 Novembre 1918, 69622 Villeurbanne Cedex, France.

[3] To whom correspondence should be addressed. Fax: (91)-231-656133.

1064-7562/98/0100-0037$15.00/0

the transparency ratio (TR) of direct to hemispherical transmittance in the case of window insulation applications. In order to minimize the scattering effects, the fabrication of large silica aerogel monoliths by the sol-gel mehod has become a major ambition of many research groups [4–6] all over the world for a decade. Some authors [7–9] used optical measurement techniques as a tool for a better understanding of the structure of silica aerogels, and light-scattering results are very efficient for describing and modeling it using the fractal theory. A research group led by Arlon J. Hunt at the University of California, Berkeley, has been developing various techniques [10] to produce commercially viable porous transparent aerogels and investigating their properties for insulating applications, since 1982. Also, there has been much research work in Western Europe on translucent window systems using aerogels between two sheets of glass [11, 12]. These would be useful for passive solar energy utilization in buildings [13, 14], for heat insulation [15], and for certain applications in bringing daylight into areas that do not receive direct light. Although significant improvements to the sol-gel process were realized, further research is required to develop transparent silica aerogels to the point of commercialization. So, in order to tailor the properties and to produce silica aerogels with high direct transmittance and low diffusive values, for the above-mentioned applications, systemic and detailed experiments were carried out on the effect of the molar ratios of catalyst (ammonia), solvent (methanol), and water to precursor (tetramethoxysilane) on the optical properties of resulting aerogels. Most of our present investigations reveal that the spectra measured with spectrophotometers on relevant series of samples have been used to test the sensibility of the transmittance and scattering to several sol-gel processing parameters. The optical data, together with the porosity measurements, allowed us to improve the process toward the fabrication of silica aerogels with a low diffusive transmittance and low index of refraction.

2. EXPERIMENTAL

2.1. Sample Preparation

Silica alcogel was prepared by hydrolyzing tetramethoxysilane (TMOS) in methanol (MeOH), catalyzed by ammonia (NH_4OH), yielding monosilicic acid:

$$Si(OCH_3)_4 + 4H_2O \rightarrow Si(OH)_4 + 4CH_3OH \quad (1)$$

The monosilicic acid is unstable and hence condenses to produce silica alcogel.

$$nSi(OH)_4 \rightarrow nSiO_2 + 2nH_2O \quad (2)$$

The methanol present in the pores was then removed by supercritical drying method. The controlled evacuation of the methanol solvent was done above the critical point of methanol where no solvent/vapor interface exists to create surface tension that would collapse the SiO_2 network. The details of the autoclave and pressure–temperature cycles were given in our recent publication [16]. The resulting aerogel has a low density (ρ_b) and a high porosity (volume fraction is air).

2.2. Spectrophotometric Measurements and Integrating Sphere Geometry

To characterize the transparency of silica aerogels made of various molar ratio combinations of TMOS, MeOH, H_2O, and NH_4OH, optical measurements were performed with a Beckmann 5240 UV–Visible–NIR spectrophotometer equipped with an integrating sphere, which covered a wavelength range of 300 to 2500 nm. This equipment produces spectra of the normal-hemispherical (direct + diffuse) transmittance with a stated accuracy of ± 15 nm (Fig. 1a). Throughout our measurements, the incident light was made to fall normally onto the aerogel sample surface to prevent Fresnel specular reflection. The integrating sphere was kept behind the sample for the detection of transmitted light. Integrating sphere geometry was used to measure the normal (n)-diffuse or normal (n)-hemispherical transmittance characteristics of the aerogel sample. It has two ports, namely, entrance and exit ports, along the diagonal. First, the aerogel under investigation was placed at the entrance port, letting the exit port open (Fig. 1b). This detected only the n-diffuse transmittance component, while the n-direct component of transmission was lost through the exit port. Second, the exit port of the integrating sphere was blocked by a suitable reflection standard and the detector measured the n-hemispherical transmittance, which includes both diffuse and direct components (Fig. 1c). The n-direct transmittance was determined by subtracting the diffuse from the hemispherical transmittance. Further details of transmittance measurements and integrating sphere theory are given in Refs. 17 and 18. For some selected samples, the direct-to-hemispherical transmittance ratio (TR) and solar energetic transparencies were also measured. The TR was calculated using the formula

$$TR = (\tau^{nh} - \tau^{nd})/\tau^{nh} \quad (3)$$

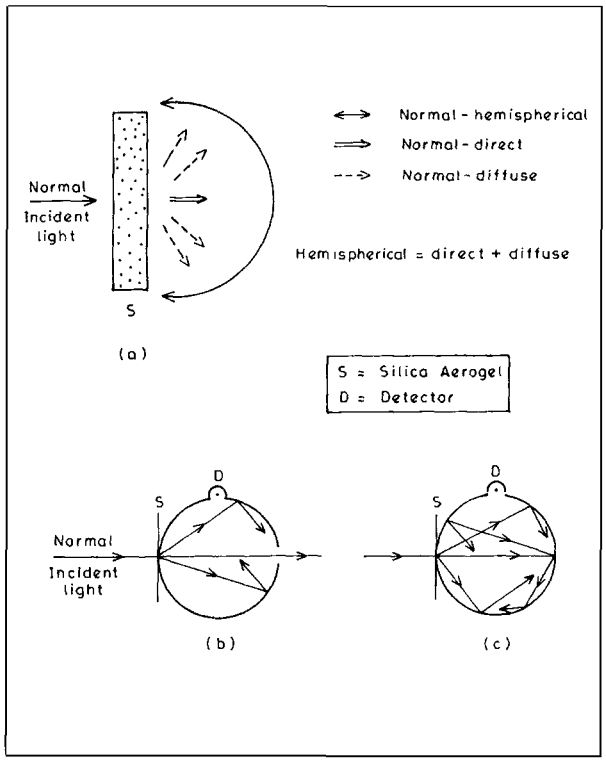

Fig. 1. (a) Representation of normal-hemispherical (direct + diffuse) transmittance through a silica aerogel sample. (b) Measurement of normal-diffuse and (c) measurement of normal-hemispherical components of transmittance using the integrating sphere technique.

where τ^{nh} and τ^{nd} are the n-hemispherical and n-diffuse components of the transmittance, respectively.

2.3. Other Methods of Characterization

Pore size distributions (PSDs) were measured using a multiple-point nitrogen gas adsorption BET surface analyzer (Model ASAP 2000) made by Micromeritics. In this method, first the aerogel samples were degassed in vacuum at 400°C and then a flowing mixture of carrier gas (He) and an adsorbate gas (N_2) was passed through a glass cell containing the sample. A BET analysis from the amount of N_2 gas adsorbed at various partial pressures ($0.05 < p/p_o < 0.3$, N_2 molecular cross sectional area = 16.2 Å^2) was used to determine the surface area. PSDs were calculated from the desorption isotherms using the Kelvin equation.

$$\ln\left[\frac{p}{p_0}\right] = \left[\frac{-2\gamma V}{rRT}\right] \tag{4}$$

which establishes the relationship between the pore radius (r) and the relative pressure (p/p_0) employed in the N_2 adsorption–desorption technique. The symbols V and γ represent the molar volume and the surface tension of the condensed liquid (N_2) in the pores. The bulk densities (ρ_b) of all the aerogels were also measured from their weights, whose dimensions were determined by a traveling microscope. The percentage of porosity was obtained using the relation

$$P = 1 - (\rho_b/\rho_s) \tag{5}$$

where ρ_s is the skeletal density of silica aerogel measured by the He pycnometer (Quantachrome) and its value was found to be 1900 kg m^{-3}. The pore volume (V_p) was calculated from the formula

$$V_p = \frac{1}{\rho_b} - \frac{1}{\rho_s} \tag{6}$$

where ρ_b and ρ_s are the bulk and skeletal densities of the aerogels, respectively.

3. RESULTS AND DISCUSSION

It is well-known that an isolated spherical particle behaves as a Rayleigh scatterer if its radius, r, is much less than $\lambda/2\pi n$, where λ is the vacuum wavelength of the incident and scattered light and n is the index of refraction of the particle. The scattered intensity from this particle for an incident light of unit intensity is given by

$$I = \frac{8\pi^4 r^6}{d^2\lambda^4}\left[\frac{n^2 - 1}{n^2 + 2}\right]^2 (1 + \cos^2\theta) \tag{7}$$

where θ is the scattering angle measured from the forward beam direction and d is the distance from the particle. The total cross section for scattering is given by integrating Eq. (7) over a large spherical surface. Hence, a spectrophotometer equipped with an integrating sphere was employed in the present study to measure the total diffusion from the particle and hemispherical transmittance of the incident light for various wavelengths. The main object of the present study actually is to minimize the diffuse transmittance part and, at the same time, increase the n-direct transmittance values to be as close as possible to the physical minimum related to the Rayleigh theory [19]. To achieve the above goal, various sol-gel processing parameters such as the molar ratios of catalyst (NH_4OH), solvent (MeOH), and water to precursor (TMOS) were varied to optimize the characteristics of the resulting aerogels. Some of the physical properties and optical transmittance values of silica aerogels in the visible region are listed in Table I.

Table I. Physical Properties and Optical Transmittance of Silica Aerogels as a Function of the Molar Ratio of TMOS : MeOH : H_2O : NH_4OH

Sample no.	Molar ratio of				Density, ρ_b (kg m^{-3})	BET surface area (m^2 g^{-1})	Porosity, P (%)	Pore volume, V_p ($\times 10^{-3}$ m^3 kg^{-1})	Direct transmittance (%) of 10-mm-thick sample at	
	TMOS	MeOH	H_2O	NH_4OH					400 nm	800 nm
1	1	12	4	3.6×10^{-6}	43	690	97.73	22.72	24	34
2	1	12	4	3.6×10^{-3}	49	1105	97.42	19.88	42	92
3	1	12	4	1.0	73	850	96.15	13.17	58	95
4	1	4	4	3.6×10^{-3}	87	875	95.42	10.96	35.5	50.1
5	1	20	4	3.6×10^{-3}	40	940	97.89	24.47	52	93
6	1	40	4	3.6×10^{-3}	32	825	98.31	30.82	57	81
7	1	12	2	3.6×10^{-3}	75	755	96.05	12.80	45	71
8	1	12	6	3.6×10^{-3}	55	940	97.10	17.65	48	92
9	1	12	10	3.6×10^{-3}	62	610	96.73	15.60	41	90
10	1	12	12	3.6×10^{-3}	74	520	96.10	12.98	36	90

Figures 2–4, 6–8, and 10–12 show the optical transmittance spectra of silica aerogels (each 10 mm thick) made of different molar ratio combinations and supercritically dried by the alcohol method. Each figure presents the n-hemispherical transmittance spectrum (curve I), the n-diffuse spectrum (curve II), and the n-direct spectrum (curve III). The peaks between 1200 and 2000 nm are due to adsorbed water and those between 2200 and 2500 nm are combinations of O–H and Si–O fundamentals. The rising part of the n-direct spectra between 300 and 800 nm is due to Rayleigh scattering [19]. The n-diffuse spectra confirm a maximum of scattering in this region. Moreover, the n-hemispherical curves also show a residual lack of transmittance in this region but gain the maximum value at and above 800 nm. This result supports other assumptions attributing the scattering to several orders of magnitude to the porosity of aerogels. The pore size distributions (PSDs) accounting

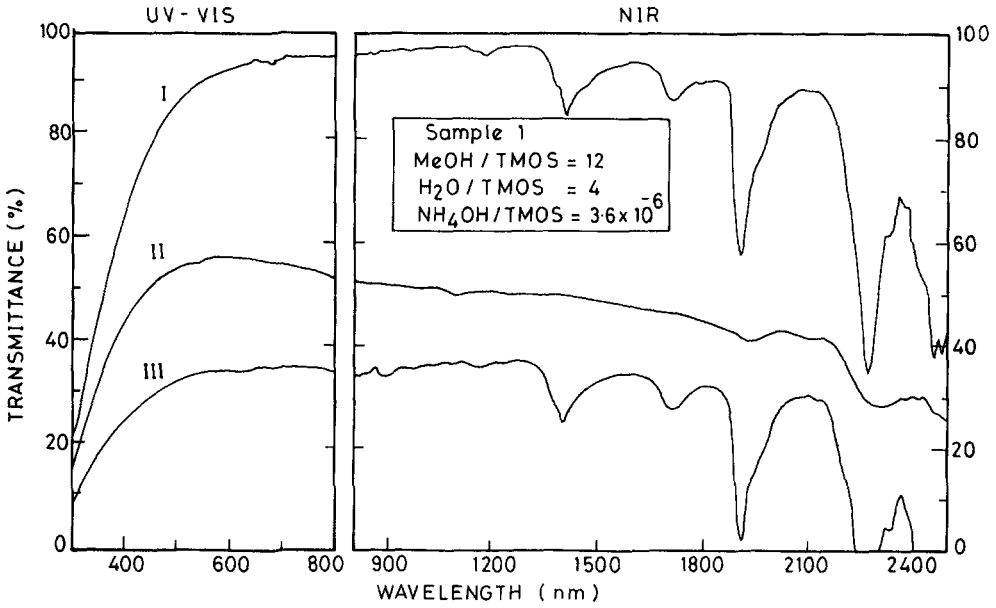

Fig. 2. UV-visible-NIR transmittance spectra obtained on an aerogel sample prepared from a NH_4OH/TMOS molar ratio of 3.6×10^{-6}. (a) Normal-hemispherical transmittance; (II) normal-diffuse transmittance; (III) normal-direct transmittance.

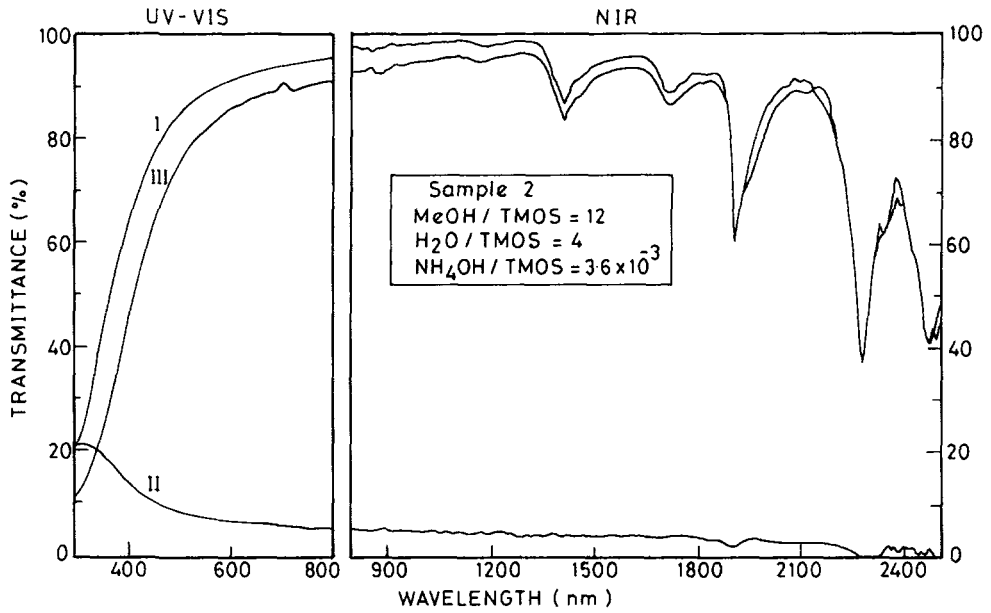

Fig. 3. UV-visible-NIR transmittance spectra obtained on an aerogel sample prepared from a NH_4OH/TMOS molar ratio of 3.6×10^{-3}. (I) Normal-hemispherical transmittance; (II) normal-diffuse transmittance; (III) normal-direct transmittance.

for the total volume of aerogels prepared by various molar ratio combinations are shown in Figs. 5, 9, and 13.

For a few silica aerogel samples (each 10 mm thick), wavelength peaks of n-diffuse trransmittance maximum (λ^{d}_{max}) were collected from the transmission spectra and are shown in Table II. Visible and solar transparencies (τ_v^{nh} and τ_s^{nh}) together with transparency ratio (TR) values are also given in Table II.

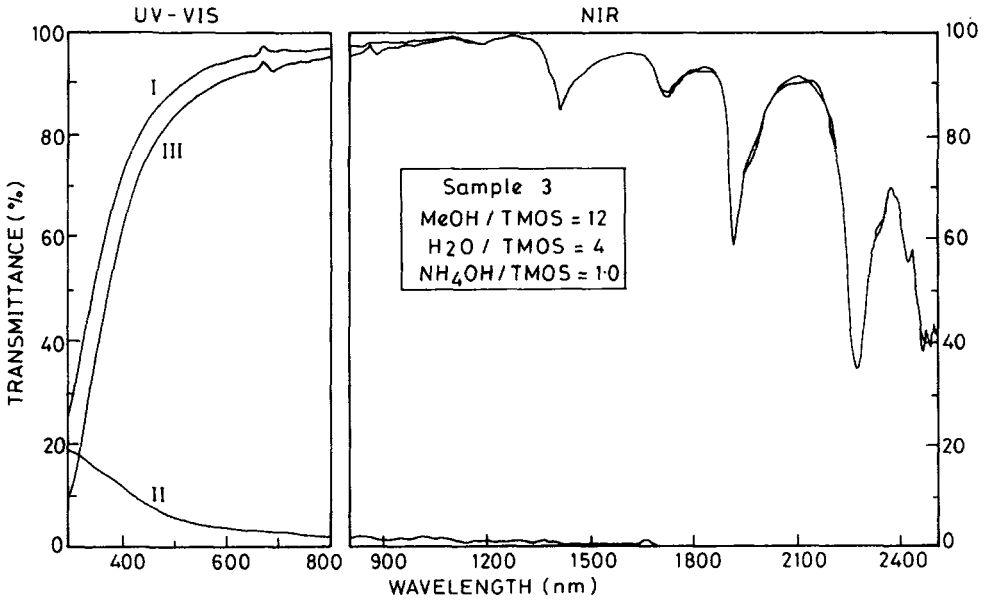

Fig. 4. UV-visible-NIR transmittance spectra obtained on an aerogel sample prepared from a NH_4OH/TMOS molar ratio of 1.0. (I) Normal-hemispherical transmittance; (II) normal-diffuse transmittance; (III) normal-direct transmittance.

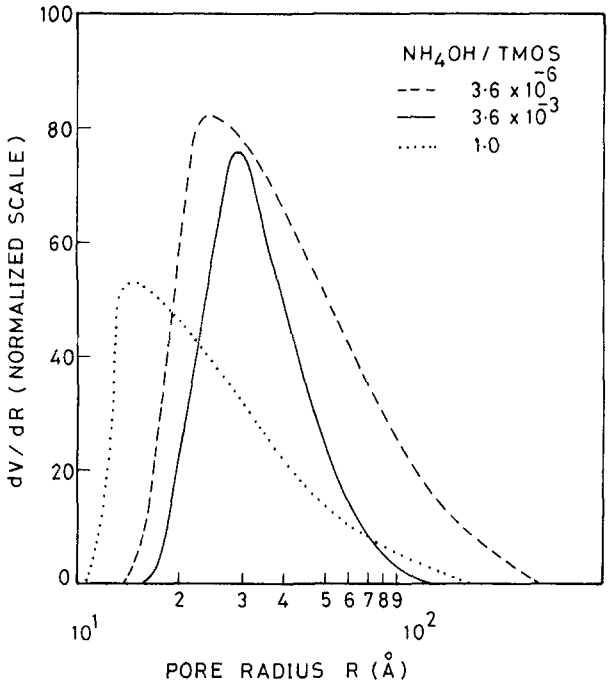

Fig. 5. Pore size distribution (PSD) for NH_4OH/TMOS = 3.6×10^{-6}, 3.6×10^{-3}, and 1.0.

3.1. Influence of the NH_4OH/TMOS Molar Ratio

Ammonia is commonly used as a catalyst in TMOS systems since it yields stable gels within suitably short reaction times, is easily extracted from the alcogel, and yields silica aerogels with very good optical properties [20]. In order to determine the influence of NH_4OH/TMOS molar ratio (A) on optical properties of silica aerogels, A values were varied from 3.6×10^{-6} to 1.0 by fixing the molar ratio of MeOH/TMOS constant at 12 and that of H_2O/TMOS at 4.

Figure 2 shows the optical transmittance spectra of silica aerogel samples prepared at an A value of 3.6×10^{-6}. It is shown that the n-diffuse transmittance curve dominates the n-direct transmittance curve, at both lower and higher wavelength region. The higher degree of scattering further indicates that the aerogels made at lower values of A ($\leq 3.6 \times 10^{-6}$) are nearly opaque in nature. This is due to the presence of an insufficient amount of catalyst for complete hydrolysis and condensation reactions, which reduces the chemical reactivity of TMOS, leading to the formation of large particle clusters and a higher percentage of void porosity. These particles act as scattering centers that are responsible for Rayleigh scattering and hence opalescence of the aerogel samples. Further, the intensity of the n-direct curve was severely affected and gave only about 24–34% transmittance in the visible region. The wavelength peak of the n-diffuse transmittance maximum (λ^{d}_{max}) was near 600 nm. But an overall finding is that the obtained aerogels for A values between 10^{-6} and 10^{-3} are semitransparent, are monolithic, and have low densities ($\rho_b \sim 45$ kg m^{-3}). The semitransparent nature of the aerogels can be an advantage in making translucent insulation for passive solar energy utilization in buildings [13, 14] and other applications that do not require transparency. But as the A value increases ($> 10^{-3}$), there is a dramatic improvement in the n-direct transmittance data. It slowly attained a maximum value of 95% in the visible region with a considerable shift of the n-diffusion peak toward shorter wavelengths (<300 nm). Figure 3 shows the transmittance spectra of the aerogel obtained for an A value of about 3.6×10^{-3}. It is clearly seen that the n-diffuse transmittance spectrum was negligible in higher

Table II. Visible and Solar Energetic Transparencies of Some Selected Silica Aerogel Samples (Thickness of Each Sample = 10 mm)

Sample no.	Volume shrinkage (%)	τ_v^{nh} (%)	λ^{d}_{max} (nm)	τ_s^{nh} (%)	TR for solar radiation (%)	Nature of the aerogel sample
1	8	87.5	600	87.9	75.1	Monolithic and opaque
2	~1–2	84.1	320	84.7	90.4	Monolithic and transparent
3	5	87.7	<300	88.1	92.5	Transparent but cracked
4	~10	89.5	480	89.9	88.8	Monolithic and semitransparent
5	<1	87.3	318	87.7	91.2	Monolithic and transparent
6	>5	89.1	~520	89.4	89.6	Transparent but cracked
7	8–10	88.0	410	88.6	81.5	Monolithic and less transparent
8	<2	83.9	319	84.5	90.9	Monolithic and transparent
9	20	85.5	<300	86.1	90.1	Transparent but cracked

wavelength regions. In the visible region, considerably less scattering was observed. The λ^{d}_{max} peak was also shifted toward the lower wavelength of ~320 nm. Silica aerogels obtained around this molar ratio ($A \sim 3.6 \times 10^{-3}$) were found to be monolithic and highly transparent (~92%) to visible light. An increase in the A value up to 3.6×10^{-3} resulted in an increase in the partial positive charge on the SiO_2 particles, creating a high repulsive barrier. Beyond this barrier limit, the particles come close together and strong linkages with a highly branched structure result. The increased connectivity between the SiO_2 particles further reduces the heterogeneity in the pore structures, leading to a much lower degree of scattering.

Figure 4 shows the transmittance spectra of the aerogel sample with an A value of 1.0. The λ^{d}_{max} peak has completely shifted toward wavelengths of <300 nm, with fairly low diffusion in the visible region. The n-direct spectrum was found to have a maximum of 95% at a wavelength of 800 nm. But the major disadvantage experienced with this molar ratio ($A \sim 1$) is that, upon supercritical drying, the gels were found to shrink and crack. The reason for cracking is that as the A value increases, the condensation reaction rate increases sharply, which abruptly stiffens the gel network. The thermal stresses developed during supercritical evaporation of the solvent creates strains and cracks in the alcogel [21].

A clearer idea of the pore sizes can be obtained from the distribution curves shown in Fig. 5, which shows the pore size distribution (PSD) of the aerogels for three different A values as a function of the differential pore volume. The PSD is generally defined as the ratio of the change in pore volume to the change in pore radius. The area under integration of these plots directly corresponds to the pore volume. It is clear from Fig. 5 that the PSD for lower values of A ($\sim 3.6 \times 10^{-6}$) is wide. This attributes to the void porosity, macropores, and ultimately the pore heterogeneity [5]. As the value of A increases ($> 3.6 \times 10^{-6}$), the rates of hydrolysis and condensation are faster, leading to a narrow PSD. The narrow PSD reduces the differential pressures during supercritical extraction of the solvent, leading to monolithic silica aerogels.

3.2. Influence of the MeOH/TMOS Molar Ratio

To study the influence of the MeOH/TMOS molar ratio (B), alcosols were prepared by fixing the molar ratio of NH_4OH/TMOS constant at 3.6×10^{-3} and that of H_2O/TMOS constant at 4. The values of B were varied from 2 to 40.

Figure 6 shows the transmittance spectra of the aerogel sample prepared by at a B value of around 4. It is clear from the figure that for lower (~4) values of B,

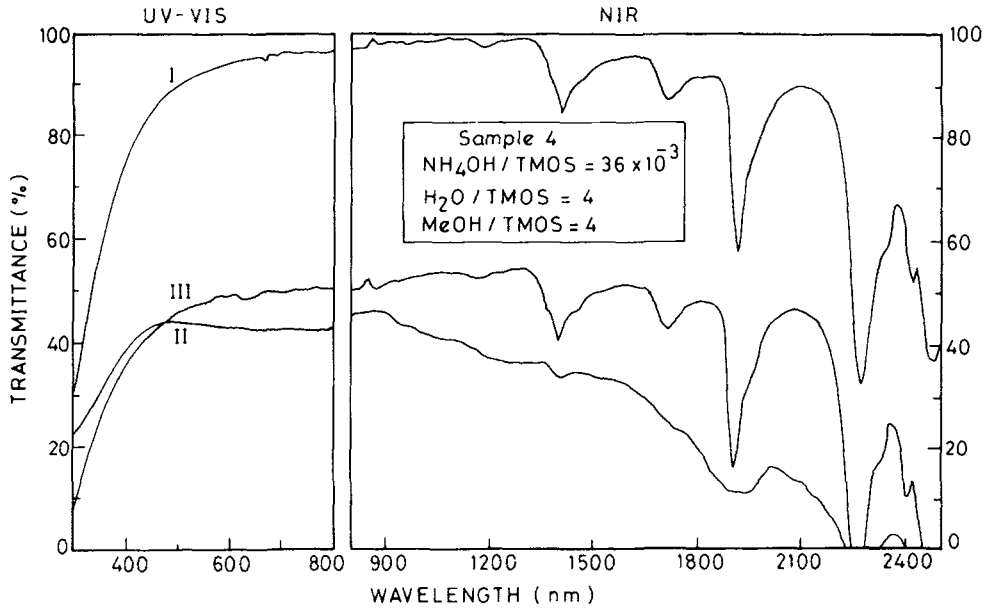

Fig. 6. UV-visible-NIR transmittance spectra obtained on an aerogel sample prepared from a MeOH/TMOS molar ratio of 4. (I) Normal-hemispherical transmittance; (II) normal-diffuse transmittance; (III) normal-direct transmittance.

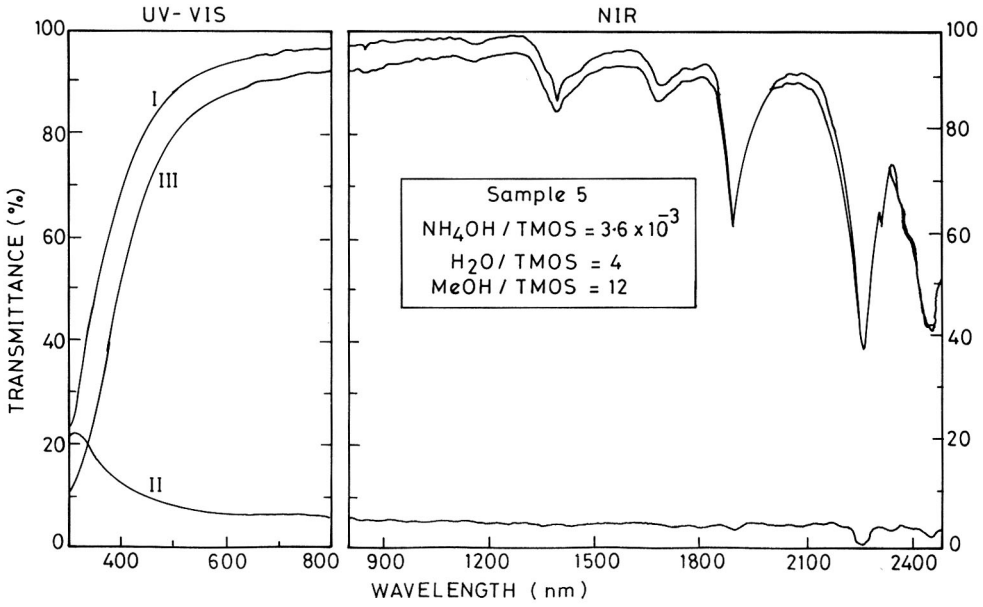

Fig. 7. UV-visible-NIR transmittance spectra obtained on an aerogel sample prepared from a MeOH/TMOS molar ratio of 12. (I) Normal-hemispherical transmittance; (II) normal-diffuse transmittance; (III) normal-direct transmittance.

the n-diffuse transmittance is prominent and is competing with the needed n-direct transmittance curve. The increase in scattering is accompanied by an increase in the λ^{d}_{max} value, which was around 480 nm. Due to this, the n-direct transmittance curve shows a maximum of only 35.5% in the visible spectrum. Although MeOH acts as a homogenizing agent to promote hydrolysis of TMOS, a much lower content of MeOH produces heterogeneity in the pore structures because of the immiscibility of TMOS and water. The heterogeneity that produces new macropores and voids increases the light-scattering nature of the silica aerogel. But an increase in the MeOH content reduces the TMOS concentration, resulting in a low oxide content in the final hydrolyzed product [22]. A B value of around 12 not only improved the n-direct transmittance up to a maximum 92% but also gave more acceptable and less prominent n-diffuse transmittance, with a sharp peak at 320 nm (see Fig. 7). Due to the shift of λ^{d}_{max} toward a wavelength of ~320 nm, the aerogel under investigation appeared to have a bluish tinge under a dark background. A slight increase in transmittance (~93% in the visible region) with a considerably low bulk density (ρ_b ~ 40 kg m^{-3}) and a low refractive index (1.0084) have been achieved for a B value of around 15. An optical transmittance of 93% in the visible region is the highest value ever reported for any porous solid material. These properties are quite suitable for the construction of Cerenkov counters in which silica aerogels can act as a radiator [1].

Figure 8 shows the transmittance spectra of a silica aerogel prepared at a higher (~40) B value. The λ^{d}_{max} peak was found to be around 520 nm. An interesting point is that as B increases beyond 40, the n-diffuse transmittance curve experiences a uniform spread instead of a peak in the visible region. This can be attributed to the farther separation of sol particles, which weakens the cross-linking and produces no significant change in the light scattering. A further increase in the B value (>40) increases the volume fraction of voids and pores with larger sizes, which gives rise to inhomogeneities in the aerogel network. Hence a less transparent (~80%) aerogel with more scattering was obtained.

Figure 9 describes the PSD of aerogels for B values of 4, 12, and 40. It is clear that for lower (~4) and higher (≥40) B values, PSD are widely separated, indicating inhomogeneity in the aerogel network, which results in a decrease in n-direct transmission. However, for a medium B value (~12), the PSD is somewhat sharp and narrow, indicating less heterogeneity of porosity and good connectivity between the particles. But it is clear that the bulk density (ρ_b) of the resulting aero-

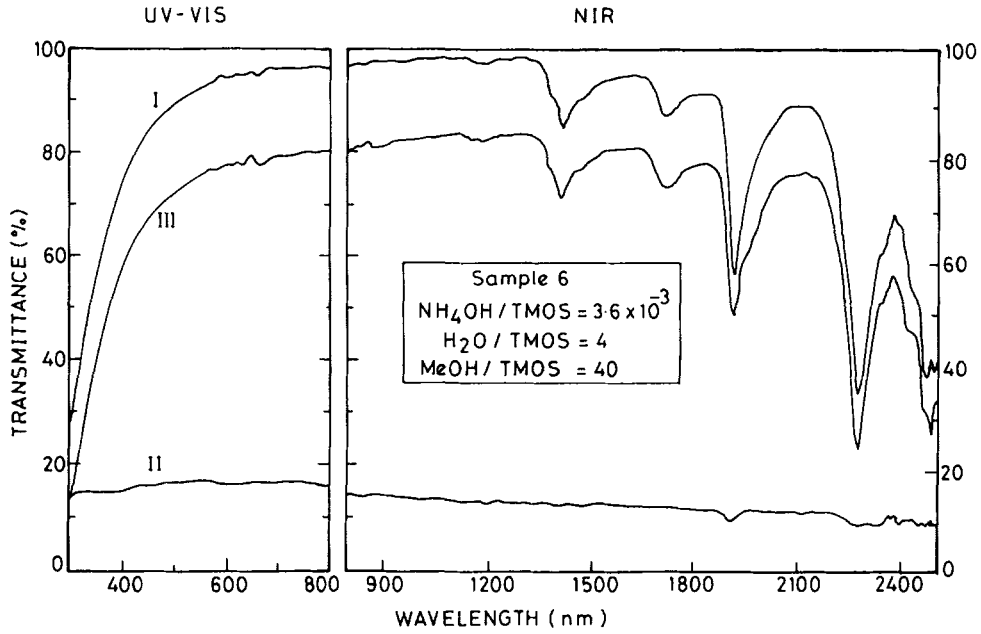

Fig. 8. UV–visible–NIR transmittance spectra obtained on an aerogel sample prepared from a MeOH/TMOS molar ratio of 40. (I) Normal-hemispherical transmittance; (II) normal-diffuse transmittance; (III) normal-direct transmittance.

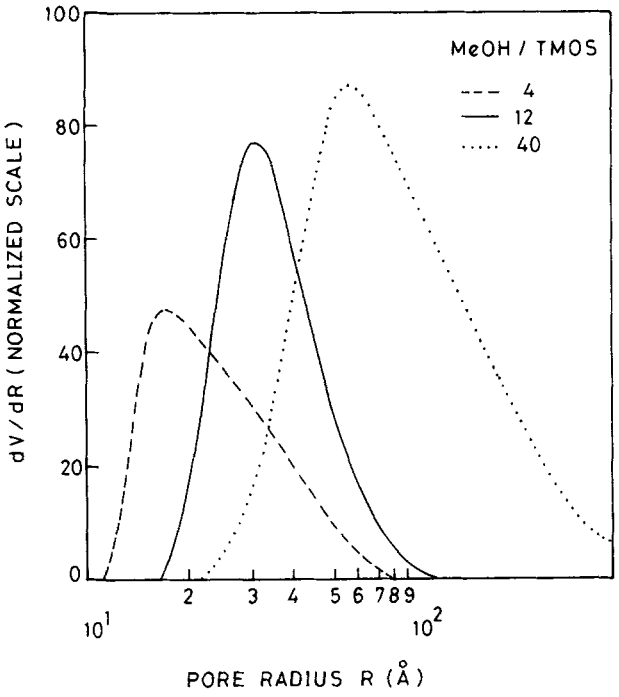

Fig. 9. Pore size distribution (PSD) for MeOH/TMOS = 4, 12, and 40.

gel is dependent solely on the amount of MeOH employed in the sol-gel process (see Table I).

3.3. Influence of the H_2O/TMOS Molar Ratio

The molar ratio of H_2O/TMOS (C) was varied from 2 to 10 by keeping the molar ratios of NH_4OH/TMOS and MeOH/TMOS constant at 3.6×10^{-3} and 12, respectively.

Figure 10 shows the spectra of the aerogel sample prepared at a C value of around 2. It is clear that for this value of C, n-direct transmittance decreased a little and a maximum of 70% was observed in the visible region. The λ^d_{max} peak was situated around 410 nm. The scattering was found to cease with an increase in wavelength. As water directly participates in the hydrolysis reaction, lower amounts of water ($C \sim 2$) resulted in a lower number of hydrolyzed monomers (Si–OH groups) with very limited cross-linking. Hence drying at the supercritical point of methanol resulted in slightly more densified ($\rho_b \sim 75$ kg m^{-3}) and less transparent (70%) silica aerogels. An increase in the amount of water enhances the gelation process, which in turn produces gels

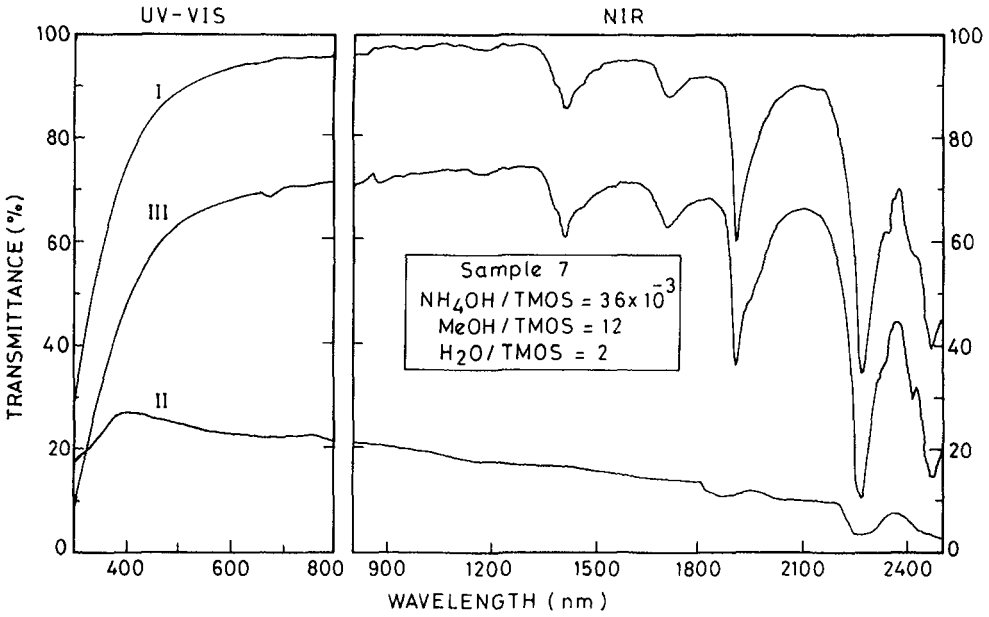

Fig. 10. UV–visible–NIR transmittance spectra obtained on an aerogel sample prepared from a H_2O/TMOS molar ratio of 2. (I) Normal-hemispherical transmittance; (II) normal-diffuse transmittance; (III) normal-direct transmittance.

with larger pore diameters. However, more condensed species and hence less diffusion transmittance were obtained for moderate values of C, between 4 and 5. The presence of a stoichiometric amount of water ($C \sim 4$) hydrolyzes all the alkoxide groups, leading to the formation of a highly branched tridimensional polymeric network with interstitial pores. Figure 11 shows the transmittance spectra of an aerogel prepared at a mod-

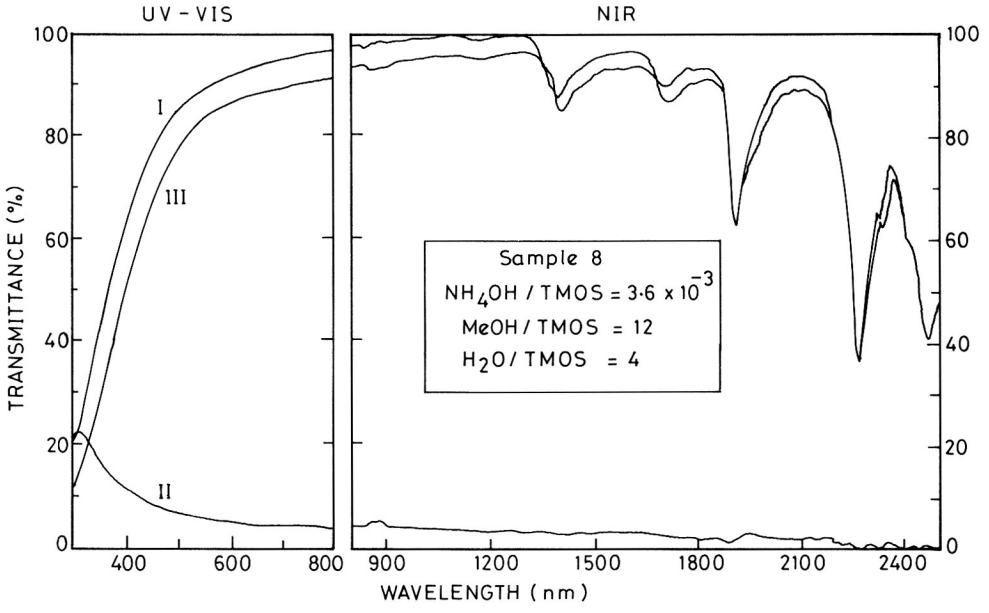

Fig. 11. UV–visible–NIR transmittance spectra obtained on an aerogel sample prepared from a H_2O/TMOS molar ratio of 4. (I) Normal-hemispherical transmittance; (II) normal-diffuse transmittance; (III) normal-direct transmittance.

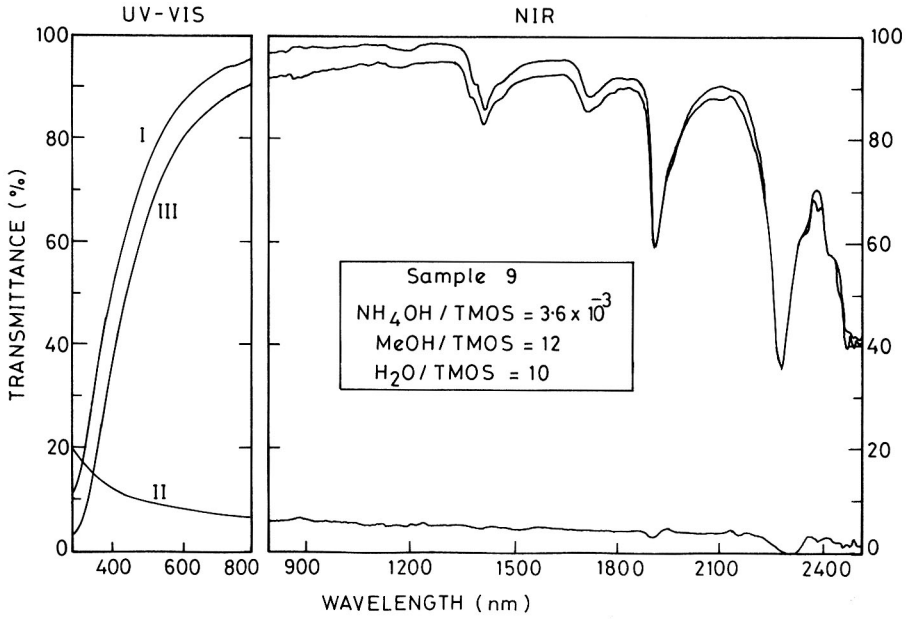

Fig. 12. UV-visible-NIR transmittance spectra obtained on an aerogel sample prepared from a H_2O/TMOS molar ratio of 10. (I) Normal-hemispherical transmittance; (II) normal-diffuse transmittance; (III) normal-direct transmittance.

erate value of C, ~4. The n-diffused transmittance was reduced to less tahn 5%, while the n-direct transmittance was enhanced to greater than 92% at 800 nm. The

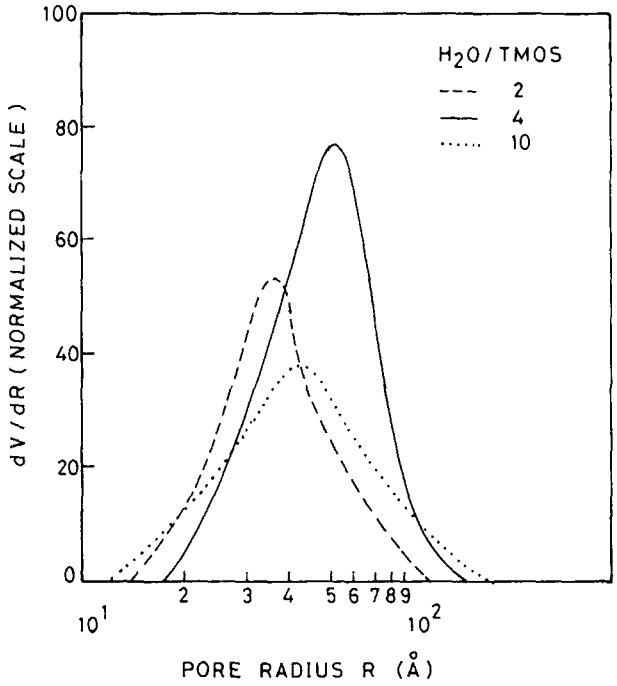

Fig. 13. Pore size distribution (PSD) for H_2O/TMOS = 2, 4, and 10.

λ^d_{max} peak was found at 319 nm with around 24% diffusion. Use of an excess amount of water ($C > 5$) increased the final texture of the aerogel product. Even though good cross-linking between siloxane chains exists, the excess water present in the alcogel causes shrinkage and cracks in the aerogel during the supercritical drying process. This resulted in more densified ($\rho_b \approx 74$ kg m^{-3}) but highly transparent (~90% at 800 nm) silica aerogels. The optical transmittance of such an aerogel made at $C = 10$ is shown in Fig. 12. The high n-direct transmittance is due to the complete shift of the λ^d_{max} peak below 300 nm. The scattering was also minimum due to less heterogeneity in the pore structures.

The variation in PSD of the aerogels for three C values (2, 4, 10) is represented in Fig. 13. It is clear from the figure that at lower (~2) and higher (~10) C values, the PSD shifted to a smaller radius of the pores, whereas for medium C values (~4), the PSD was narrow and shifted to a larger but uniform pore radius. These results support the optical transmittance of silica aerogels as a function of C values as described in the above discussion.

4. CONCLUSIONS

Silica aerogels with different optical transmittance values have been obtained by systematically varying the

molar ratios of NH_4OH, MeOH, and H_2O to TMOS. It has been found that higher molar ratios of NH_4OH/TMOS ($>10^{-3}$), MeOH/TMOS (>20), and H_2O/TMOS (>10) resulted in high-density (70–75 kg m^{-3}), transparent (90–95% in the visible region) but cracked aerogels. But very low molar ratios of these combinations gave monolithic, low-density (40–70 kg m^{-3}), and semitransparent (35–70%) aerogels, which can be used in translucent window systems. A good optical-quality aerogel with ~93% direct transmittance and a low density (~45 kg m^{-3}) was obtained with the molar ratio combination of 1 TMOS : 12 MeOH : 4 H_2O : 3.6×10^{-3} NH_4OH, which can be used for Cerenkov radiation detection. Apart from these, visible and solar energetic transparencies together with the transparency ratio (TR) for a few aerogel samples were also measured and reported.

ACKNOWLEDGMENTS

The financial support received from the Department of Science and Technology (DST), Government of India, under the research project [No. III 5(21)/92-ET] on "Silica Aerogels" is gratefully acknowledged. Two of the authors (D.H. and P.B.W.) are grateful to the DST for Senior Research Fellowships. A.V.R. is most grateful to the Academy of Lyon, University Claude Bernard, Lyon I, France, for a visiting professorship.

REFERENCES

1. M. Cantin, M. Casse, L. Koch, R. Jouan, P. Mestreau, D. Roussel, F. Bonnin, J. Moutel, and S. J. Teichner, *Nucl. Instr. Meth.* **118,** 117 (1974).
2. M. Bourdinaud, J. B. Cheze, and J. C. Thevenin, *Nucl. Instr. Meth.* **136,** 99 (1976).
3. K. E. Johansson, J. Norrby, and J. P. Lagnaux, *Nucl. Instr. Meth.* **154,** 253 (1978).
4. G. Poelz and R. Riethmuller, *Nucl. Instr. Meth.* **195,** 491 (1982).
5. A. Venkateswara Rao, G. M. Pajonk, N. N. Parvathy, and E. Elaloui, in *Sol-Gel Processing and Applications*, Y. A. Attia, ed. (Plenum, New York, 1994), p. 237.
6. A. J. Hunt and P. Berdahl, *MRS Symp. Proc.* **32,** 275 (1985).
7. P. Lourdin, J. Appell, J. Pelous, and T. Woignier, *Proc. 2nd ISA, Rev. Phys. Appl., C4-197, Ed. Physique* (1989).
8. P. Wang, W. Korner, A. Emmerling, A. Becs, J. Kuhn, and J. Fricke, *J. Non-Cryst. Solids* **145,** 141 (1992).
9. A. Beck, O. Gelsen, P. Wang, and J. Fricke, *Proc. 2nd ISA, Rev. Phys. Appl., C4-203, Ed. Physique* (1989).
10. A. J. Hunt and M. Martin, *Proc. 3rd ISA*, Wurzberg (1991).
11. K. I. Jensen, *J. Non-Cryst. Solids* **145,** 237 (1992).
12. V. Wittwer, *J. Non-Cryst. Solids* **145,** 233 (1992).
13. D. Buttner and J. Fricke, *Int. J. Sol. Energy* **3,** 89 (1985).
14. R. Caps and J. Fricke, *Sol. Energy* **36,** 361 (1986).
15. E. Schreiber, E. Boy, and K. Bertsch, *Proc. 1st ISA*, Wurzberg (1985).
16. A. Venkateswara Rao, G. M. Pajonk, and N. N. Parvathy, *J. Mater. Sci.* **29,** 1807 (1994).
17. W. W. Wendlandt and H. G. Hecht, *Reflectance Spectroscopy* (Interscience, New York, 1996).
18. CIE TC-2.3, Technical Report on Absolute Reflectance Measurements (1979).
19. M. Rubin and C. M. Lambert, *Sol. Energy Mat.* **7,** 393 (1993).
20. J. C. Pouxviel, J. P. Boilot, J. C. Beloeil, and J. Y. Lallemand, *J. Non-Cryst. Solids* **89,** 345 (1987).
21. G. W. Scherer, *J. Non-Cryst. Solids* **145,** 33 (1992).
22. B. E. Yoldas, *J. Non-Cryst. Solids* **82,** 11 (1986).